

A Geometric Embedding Approach to Multiple Games and Multiple Populations

Bastian Boll^{1*}, Jonas Cassel¹, Peter Albers¹, Stefania Petra²,
Christoph Schnörr¹

¹Institute for Mathematics, Heidelberg University, Im Neuenheimer Feld
205, Heidelberg, 69120, Baden-Württemberg, Germany.

²Institute for Mathematics, Augsburg University, Universitätsstraße 2,
Augsburg, 86159, Bavaria, Germany.

*Corresponding author(s). E-mail(s): bastian.boll@iwr.uni-heidelberg.de;

Abstract

This paper studies a meta-simplex concept and geometric embedding framework for multi-population replicator dynamics. Central results are two embedding theorems which constitute a formal reduction of multi-population replicator dynamics to single-population ones. In conjunction with a robust mathematical formalism, this provides a toolset for analyzing complex multi-population models. Our framework provides a unifying perspective on different population dynamics in the literature which in particular enables to establish a formal link between multi-population and multi-game dynamics.

Keywords: Replicator dynamics, Assignment Flows, Manifold Embedding, Information Geometry

Contents

1	Introduction	2
1.1	Overview, Contribution	2
1.2	Organization	4
1.3	Basic Notation	4
2	Preliminaries	4
2.1	Fisher-Rao Geometry, Replicator Dynamics	4

2.2 Data Labeling and Assignment Flows	6
3 Embedding the Assignment Manifold	7
4 Multiple Populations and Multiple Games	10
5 Tangent Space Parameterization	12
6 Learning Replicator Dynamics from Data	13
7 Asymptotic Behavior	15
8 Conclusion	18
A Additional Lemmata	25
B Proofs	27
B.1 Proof of Theorem 3.1	27
B.2 Proof of Proposition 3.2	29
B.3 Proof of Lemma 3.3	30
B.4 Proof of Theorem 3.5	30

1 Introduction

1.1 Overview, Contribution

Evolutionary game theory (Hofbauer and Sigmund, 1998; Sandholm, 2010) is an established framework for modeling problems in diverse areas ranging from mathematical biology (Smith and Price, 1973; Smith, 1982; Hammerstein and Selten, 1994; Nowak, 2006; Leimar and McNamara, 2023) to economics (Gardner, 2003; Samuelson, 2016). It assumes a dynamic perspective on games played by a large and well-mixed population of agents. In this context, the earliest dynamical model of population state is the *replicator equation* (Taylor and Jonker, 1978; Schuster and Sigmund, 1983), which has since been generalized in several ways (Bednar and Page, 2007; Cressman and Tao, 2014) to accommodate more complex situations.

This paper provides an embedding approach for studying the following two classes of scenarios within a single framework.

- *Multi-population dynamics* model multiple interacting populations or species. The state space is a product manifold of multiple simplices, and payoff may depend on the state of all populations. The resulting dynamics are multiple coupled replicator dynamics on the product manifold of multiple simplices.
- *Multi-game dynamics* model agents that simultaneously play multiple games, earning cumulative payoff. The state space is a single simplex with dimension growing exponentially in the number of games. Interaction between games occurs whenever the population state is outside of a specific submanifold.

Here, we study an embedding of multiple probability simplices into a combinatorially large simplex of joint distributions. As further detailed in Section 8, our approach is closely related to *Segre embeddings* of projective spaces (Görtz and Wedhorn, 2020) which play a prominent role in many areas of mathematics and physics, such as *independence models* in algebraic statistics (Drton et al, 2009) and *entanglement* in quantum mechanics (Bengtsson and Życzkowski, 2017). Based on this Ansatz, we develop a geometric perspective and formalism to study the relationship between replicator dynamics of multiple populations and multi-game replicator dynamics. In particular, we demonstrate that the multi-game dynamics of Hashimoto (2006) share a generic payoff structure with multi-population games.

Our work further constitutes a formal reduction of multi-population dynamics to – a much higher-dimensional – single-population dynamics, which is helpful for theoretical analysis. We demonstrate this by transferring two results on the asymptotic behavior of replicator dynamics from the single-population to the multi-population setting.

Concerning applications, our work aims to provide insight into the structure of multi-population and multi-game dynamics, along with a robust mathematical toolset for domain experts to analyze complex systems. Indeed, there is a growing need for more powerful dynamical models in emerging applications. For instance, Venkateswaran and Gokhale (2019) argue for the use of generalized replicator dynamics to model interactions in nature – considering multi-player interaction in a multi-game setting.

The present paper also extends our previous work on *assignment flows* (Aström et al, 2017; Schnörr, 2020). They are dynamical systems that leverage interaction along edges of a graph \mathcal{G} to infer an assignment of class labels to the nodes of \mathcal{G} from node-wise data. Applications include structured prediction problems such as semantic image segmentation in supervised (Sitenko et al, 2021) and unsupervised scenarios (Zisler et al, 2020; Zern et al, 2020).

In (Boll et al, 2021), we have shown that assignment flows can be seen as multi-population replicator dynamics and studied how payoff is transformed by embedding the state space into a single simplex of joint distributions. In the present work, we generalize this analysis to nonlinear payoff functions and provide a careful study of the involved manifolds.

We also highlight previous findings on assignment flows and their relevance to the evolutionary game theory community. In particular

- Zern et al (2022) present an exhaustive study of conditions under which certain assignment flows converge to integer assignments. These are states in which only a single played strategy remains in each population.
- Zeilmann et al (2020) have proposed a generically applicable framework for geometric numerical integration which scales to large replicator dynamics.
- Hühnerbein et al (2021); Zeilmann et al (2023) have studied methods of learning the parameters that generate replicator dynamics from data.

1.2 Organization

Section 2 contextualizes assignment flows as multi-population replicator dynamics and establishes related notation. Section 3 describes the proposed meta-simplex concept and related geometric notions as well as the embedding theorems 3.1 and 3.5, which constitute the main results of the present work. Section 4 gives three examples of dynamics considered in prior work and establishes their relationship through the lens of the geometric embedding theorems. Section 5 recapitulates a tangent space parameterization of replicator dynamics from the literature on assignment flows and studies it in the context of geometric embedding. Section 6 highlights previous findings on parameter learning for assignment flows. Section 7 demonstrates how the proposed formal reduction of multi-population to single-population dynamics can be used as a tool for formal analysis of asymptotic behavior. Section 8 gives an outlook on current assignment flow developments and concludes the paper.

The present work substantially extends the conference paper (Boll et al, 2021) in the following ways:

- The submanifold of embedded multi-population states is identified as a generalized Wright manifold and its geometry is analyzed (Theorem 3.1).
- The embedding theorem of multi-population replicator dynamics is generalized to nonlinear payoff functions (Theorem 3.5).
- Multi-game dynamics are studied as embedded multi-population replicator dynamics (Section 4).
- Tangent space parameterization of replicator dynamics is studied in the context of geometric embedding (Theorem 5.2).

1.3 Basic Notation.

For $k \in \mathbb{N}$ we use the shorthands $[k] := \{1, \dots, k\} \subset \mathbb{N}$ and $\mathbf{1}_k := (1, \dots, 1)^\top \in \mathbb{R}^k$. Angle brackets $\langle \cdot, \cdot \rangle$ are used for both the standard inner product between vectors and the Frobenius inner product between matrices. The Kronecker product of matrices (Graham, 1981) is denoted by $A \otimes B$. Componentwise multiplication of vectors x and y is denoted by $x \diamond y$, and by $\frac{x}{y}$ the componentwise division of a vector x by a strictly positive vector y . Likewise, logarithms and exponentials of vectors apply componentwise. For vectors $x \in \mathbb{R}^c$, the expression $x \geq 0$ denotes $x_i \geq 0$ for all $i \in [c]$.

2 Preliminaries

2.1 Fisher-Rao Geometry, Replicator Dynamics

In matrix games, players from a large population engage in two-player interactions. For simplicity, we assume that each player chooses from a constant set of c strategies. The payoff for a two-player interaction is then given by a $c \times c$ payoff matrix B . If players change their strategy to imitate other players with more effective strategies, the overall distribution $p \in \mathcal{S}_c$ of strategies in the population changes over time according

to the well-known *replicator dynamics*

$$\dot{p}(t) = R_{p(t)}[Bp(t)], \quad p(0) = p_0 \in \mathcal{S}_c, \quad (1)$$

where

$$\mathcal{S}_c = \{p \in \mathbb{R}^c : \langle \mathbf{1}_c, p \rangle = 1, p > 0\} \quad (2)$$

denotes the relative interior of the probability simplex with c vertices and

$$R_p = \text{Diag}(p) - pp^\top \quad (3)$$

is called the *replicator operator*. We regard \mathcal{S}_c as a Riemannian manifold with trivial tangent bundle

$$T\mathcal{S}_c \cong \mathcal{S}_c \times T_0\mathcal{S}_c, \quad T_0\mathcal{S}_c = \{v \in \mathbb{R}^c : \langle \mathbf{1}_c, v \rangle = 0\} \quad (4)$$

and equipped with the *Fisher-Rao metric*

$$\langle \cdot, \cdot \rangle_g : T_p\mathcal{S}_c \times T_p\mathcal{S}_c \rightarrow \mathbb{R}, \quad (u, v) \mapsto \left\langle \frac{u}{p}, v \right\rangle. \quad (5)$$

The barycenter of \mathcal{S}_c is denoted $\mathbf{1}_\mathcal{S} = \frac{1}{c}\mathbf{1}_c$. Vectors in \mathbb{R}^c are projected onto the tangent space $T_0\mathcal{S}_c$ by the linear map

$$\Pi_0 : \mathbb{R}^c \rightarrow T_0\mathcal{S}_c, \quad v \mapsto \Pi_0 v = v - \frac{1}{c}\langle \mathbf{1}_c, v \rangle \mathbf{1}_c. \quad (6)$$

The manifold \mathcal{S}_c has dimension $c - 1$. Two coordinate charts are particularly relevant to the following discussion. A point $p \in \mathcal{S}_c \subseteq \mathbb{R}^c$ has m -coordinates μ with

$$p = (\mu, 1 - \langle \mathbf{1}_{c-1}, \mu \rangle), \quad \mu \in \mathbb{R}^{c-1}, \quad \mu > 0, \quad \langle \mu, \mathbf{1}_{c-1} \rangle < 1 \quad (7)$$

and e -coordinates θ with

$$p = \frac{1}{Z(\theta)} \exp \left(\begin{array}{c} \theta \\ -\langle \theta, \mathbf{1}_{c-1} \rangle \end{array} \right), \quad \theta \in \mathbb{R}^{c-1}, \quad (8)$$

where $Z(\theta)$ normalizes the vector on the right-hand side such that $p \in \mathcal{S}_c$, as defined by (2). The e -coordinates θ are unconstrained and define a *global* chart for \mathcal{S}_c .

For general references to Riemannian geometry, we refer to (Lee, 2018; Jost, 2017). For references to *information geometry* which underlies the above definitions, see (Amari and Nagaoka, 2007; Ay et al, 2017).

The mean payoff in a population with state p is $\langle p, Bp \rangle$. In particular, if B is symmetric $Bp = \frac{1}{2}\partial_p \langle p, Bp \rangle$, then it is well known that (1) is the Riemannian gradient ascent flow of mean payoff with respect to the metric (5). With an eye toward numerical computation, a useful object is the *lifting map*

$$\exp_p : T_0\mathcal{S}_c \rightarrow \mathcal{S}_c, \quad \exp_p(v) = \frac{p \diamond \exp(v)}{\langle p, \exp(v) \rangle}. \quad (9)$$

It can be shown that

$$\exp_p = \exp_p \circ \Pi_0, \quad (10)$$

with the projection Π_0 given by (6), such that \exp_p is well-defined on \mathbb{R}^c . Furthermore, the mapping (9) is a first-order approximation to the Levi-Civita geodesics on \mathcal{S}_c (Aström et al, 2017). It is also closely related to the e -geodesics of information geometry (Amari and Nagaoka, 2007).

2.2 Data Labeling and Assignment Flows

We have studied dynamics similar to (1) for *data labeling* on graphs. Given a graph $\mathcal{G} = (\mathcal{V}, \mathcal{E})$ and data on each node, the task is to infer node-wise classes. For example, in image segmentation, the graph may be a grid graph of image pixels, and pixel-wise data lives in some feature space, most basically a color space. Another example is node-wise classification of citation graphs such as (Bollacker et al, 1998). Here, nodes are academic papers and edges between them denote citations. The task is to classify the topic of papers from node-wise features and citations.

In each case, graph connectivity is crucial information and a natural approach is to facilitate interaction along graph edges to inform the labeling process. We further abstract from the raw feature space of given data by lifting to a probability simplex \mathcal{S}_c on each node. The resulting state lives in the product manifold

$$\mathcal{W} = \mathcal{S}_c \times \dots \times \mathcal{S}_c \quad (11)$$

containing $n = |\mathcal{V}|$ copies of \mathcal{S}_c which we call *assignment manifold*. For $S \in \mathcal{W}$, let \mathcal{R}_S denote the operator which applies R_{S_i} on each node $i \in [n]$. Similarly, let

$$\exp_S(V), \quad V \in T_0\mathcal{W} = (T_0\mathcal{S}_c)^n \quad (12)$$

denote the map which applies (9) separately on each node, whose domain can be extended

$$\exp_S: \mathbb{R}^{n \times c} \rightarrow \mathcal{W}. \quad (13)$$

due to (10). We will still call these objects *replicator operator* and *lifting map*, respectively. Likewise, the projection

$$\Pi_0: \mathbb{R}^{n \times c} \rightarrow T_0\mathcal{W} \quad (14)$$

applies separately the mapping (6) on each node and the barycenter of \mathcal{W} reads $\mathbf{1}_{\mathcal{W}} = \frac{1}{c} \mathbf{1}_{n \times c}$.

By defining a payoff function

$$F: \mathcal{W} \rightarrow \mathbb{R}^{n \times c} \quad (15)$$

which has the state $S_i, S_j \in \mathcal{S}_c$ of nodes $i, j \in [n]$ interact exactly if $ij \in \mathcal{E}$, we have found a natural inference dynamic on \mathcal{G} given by

$$\dot{S}(t) = \mathcal{R}_{S(t)}[F(S(t))], \quad S(0) = S_0, \quad (16)$$

whose solution is called *assignment flow*. For labeling, payoff functions are designed such that the state S is driven towards an extremal point of the set \mathcal{W} . These states unambiguously associate each node with a single class. From a game-theoretical perspective, the extremal points of \mathcal{W} are states in which only a single strategy is played in each population. A more detailed overview can be found in the original work (Aström et al, 2017) and the survey (Schnörr, 2020).

3 Embedding the Assignment Manifold

In our previous work (Boll et al, 2021), we showed that assignment flows can be seen as multi-population replicator dynamics. Furthermore, we introduced a preliminary formalism for embedding the state space of multi-population dynamics into a *single*, much higher-dimensional *meta-simplex* of joint distributions. Assuming again the data labeling perspective introduced in Section 2.2, one may enumerate all c^n possible assignments of c classes to n graph nodes. This enumeration represents data labeling as a single decision between

$$N = c^n \quad (17)$$

alternatives which we view as pure strategies of a *single* population game on the meta-simplex \mathcal{S}_N .

Here, we describe a refined version of the embedding formalism as well as several additional results, generalizing and expanding our earlier findings. Note that the proposed meta-simplex \mathcal{S}_N is not to be confused with the meta-simplex concept proposed by Argasinski (2006). The latter explicitly considers the relative size of populations and has much lower dimension.

To simplify notation, we assume that agents of each population have the same number c of available pure strategies. However, the following results remain valid in more general scenarios of variable strategy sets. In addition, we index entries of vectors $p \in \mathcal{S}_N$ by multi-indices $[c]^n$ as opposed to integer indices in $[c^n]$ to improve readability. The component γ_i of a multi-index $\gamma \in [c]^n$ indexes a label $\gamma_i \in [c]$ at vertex $i \in [n]$.

We consider the following maps, defined componentwise by

$$T: \mathcal{W} \rightarrow \mathcal{T} \subseteq \mathcal{S}_N, \quad T(W)_\gamma := \prod_{i \in [n]} W_{i, \gamma_i} \quad \text{for all } \gamma \in [c]^n \quad (18a)$$

$$Q: \mathbb{R}^{n \times c} \rightarrow \mathbb{R}^N, \quad Q(X)_\gamma := \sum_{i \in [n]} X_{i, \gamma_i} \quad \text{for all } \gamma \in [c]^n \quad (18b)$$

$$M: \mathbb{R}^N \rightarrow \mathbb{R}^{n \times c}, \quad M(x)_{ij} := \sum_{\gamma \in [c]^n : \gamma_i = j} x_\gamma \quad \text{for all } (i, j) \in [n] \times [c]. \quad (18c)$$

The particular choice of these maps will be justified by laying out several compatibility properties which intricately link them to each other and to the geometries of \mathcal{W} and \mathcal{S}_N . Specifically,

- T realizes the concept of enumerating labelings in the sense that the extremal points of \mathcal{W} are bijectively mapped to the extremal points of \mathcal{S}_N .

- The restriction of M to \mathcal{T} inverts T by computing node-wise marginals. We choose the larger domain \mathbb{R}^N for M such that it becomes the adjoint mapping of Q (ref Lemma 3.4).

Theorem 3.1 (assignment manifold embedding). *The map $T: \mathcal{W} \rightarrow \mathcal{T} \subseteq \mathcal{S}_N$ is an isometric embedding of \mathcal{W} equipped with the product Fisher-Rao geometry, into \mathcal{S}_N equipped with the Fisher-Rao geometry. On its image $T(\mathcal{W}) =: \mathcal{T} \subseteq \mathcal{S}_N$, the inverse is given by marginalization*

$$M|_{\mathcal{T}} = T^{-1}: \mathcal{T} \rightarrow \mathcal{W}. \quad (19)$$

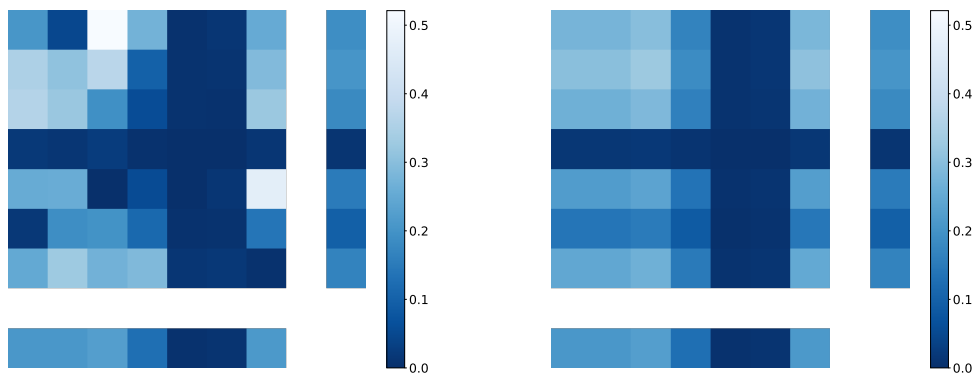
Proof. Section B.1. □

In view of the expression (18a), it is clear that \mathcal{T} is precisely the set of rank-1 tensors in $\mathcal{S}_N \subseteq \mathbb{R}^N \cong (\mathbb{R}^c)^n$. In addition, we have the following interpretation of points $T(W) \in \mathcal{T}$ within the simplex of joint distributions \mathcal{S}_N .

Proposition 3.2 (maximum entropy property). *For every $W \in \mathcal{W}$, the distribution $T(W) \in \mathcal{S}_N$ has maximum entropy among all $p \in \mathcal{S}_N$ subject to the marginal constraint $Mp = W$, with M given by (18c).*

Proof. Section B.2. □

In general, each collection of marginal distributions $S \in \mathcal{W}$ has (infinitely) many possible joint distributions. Proposition 3.2 shows that T precisely selects the least informative one among them. This situation is illustrated in Figure 1.



(a) A randomly generated joint distribution of S_1 and S_2 .

(b) The maximum-entropy joint distribution $T(S)$ of S_1 and S_2 .

Fig. 1: Marginal distributions $S = (S_1, S_2)$ and two possible conforming joint distributions. Joint distribution values are scaled by a factor of c for visual clarity.

Theorem 3.1 expresses an intricate relationship between the product Fisher-Rao geometry of \mathcal{W} and the Fisher-Rao geometry of \mathcal{S}_N . A similar compatibility is found between the lifting map (9) on \mathcal{W} and its analog on \mathcal{S}_N .

Lemma 3.3 (Lifting Map Lemma). *Let $S \in \mathcal{W}$ and $V \in \mathbb{R}^{n \times c}$. Then the mappings T, Q given by (18) satisfy*

$$T(\exp_S(V)) = \exp_{T(S)}(Q(V)), \quad (20)$$

where \exp_S on the left is given by (12) and $\exp_{T(S)}$ on the right naturally extends the mapping (9).

Proof. Section B.3. □

We will also frequently use the following useful identity connecting Q to marginalization.

Lemma 3.4 (Q Adjoint Lemma). *M and Q given by (18) are adjoint linear maps with respect to the standard inner product, i.e. for each $p \in \mathbb{R}^N$ and each $V \in \mathbb{R}^{n \times c}$ it holds that*

$$\langle p, Q(V) \rangle = \langle Mp, V \rangle. \quad (21)$$

Proof. Let $p \in \mathbb{R}^N$ and $V \in \mathbb{R}^{n \times c}$, then

$$\langle p, Q(V) \rangle = \sum_{\gamma \in [c]^n} p_\gamma Q(V)_\gamma = \sum_{\gamma \in [c]^n} p_\gamma \sum_{l \in [n]} V_{l, \gamma_l} = \sum_{l \in [n]} \sum_{j \in [c]} \sum_{\gamma_l = j} p_\gamma V_{l, \gamma_l} \quad (22a)$$

$$= \sum_{l \in [n]} \sum_{j \in [c]} V_{l, j} \sum_{\gamma_l = j} p_\gamma \stackrel{(18c)}{=} \sum_{l \in [n]} \sum_{j \in [c]} V_{l, j} (Mp)_{l, j} \quad (22b)$$

$$= \langle Mp, V \rangle. \quad (22c)$$

□

Our main result stated next is that the embedding $T: \mathcal{W} \rightarrow \mathcal{S}_N$ maps *multi*-population replicator dynamics on \mathcal{W} to *single*-population replicator dynamics on \mathcal{S}_N by a transformation of payoff functions. This generalizes our earlier finding (Boll et al, 2021) to arbitrary nonlinear payoffs.

Theorem 3.5 (Multi-Population Embedding Theorem). *For any payoff function $F: \mathcal{W} \rightarrow \mathbb{R}^{n \times c}$, the multi-population replicator dynamics*

$$\dot{W} = \mathcal{R}_W[F(W)], \quad W(0) = W_0 \quad (23)$$

on \mathcal{W} is pushed forward by T to the replicator dynamics

$$\dot{p}(t) = R_{p(t)} \hat{F}(p(t)), \quad p(0) = T(W_0), \quad \hat{F} = Q \circ F \circ M, \quad (24)$$

on \mathcal{S}_N and the map T satisfies

$$dT|_{\mathcal{W}}[\mathcal{R}_W[X]] = R_{T(W)}Q[X], \quad \text{for all } X \in \mathbb{R}^{n \times c} \text{ and } W \in \mathcal{W}. \quad (25)$$

Proof. Section B.4. □

Intuitively, the structure of \hat{F} in (24) can be seen as follows. The joint population state $p \in \mathcal{S}_N$ is first marginalized and payoff $F(Mp)$ is computed from the marginal multi-population state. Theorem 3.5 now shows that when multi-population state $W \in \mathcal{W}$ is seen as factorizing joint population state $p \in \mathcal{S}_N$ according to $p = T(W)$, then the payoff gained in state W is transformed by Q to induce replicator dynamics of the joint population state.

In the following, leading examples will be matrix games, i.e. linear payoff functions that model two-player interactions. Note, however, that Theorem 3.5 applies to arbitrary nonlinear payoff functions, including multi-player interactions.

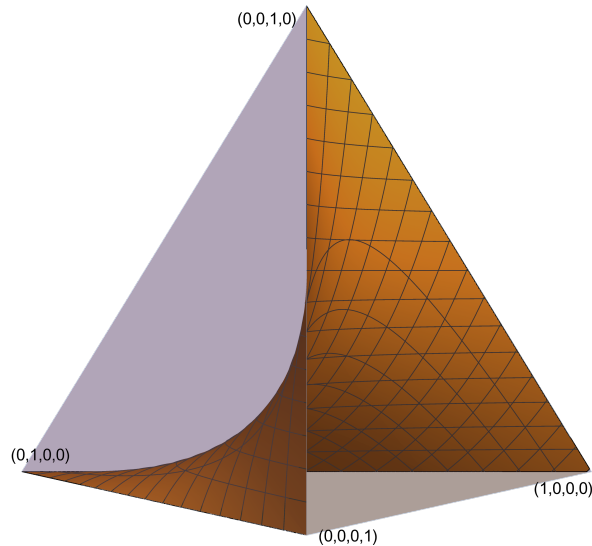


Fig. 2: The embedded submanifold $\mathcal{T} \subseteq \mathcal{S}_N$, $N = 4$. For two marginal distributions, this is known as the *Wright manifold* (Hofbauer and Sigmund, 1998, Section 18.8), (Chamberland and Cressman, 2000).

4 Multiple Populations and Multiple Games

Because both M and Q are linear operators, generalized matrix games on multiple populations reduce to simple matrix games of the joint population state exactly if the payoff F is a linear function of the multi-population state. Here, we give two examples of multi-population games, one from the assignment flow literature and one from game theory. To this end, denote by

$$s := \text{vec}_{\text{row}}(S) \in \mathbb{R}^{nc} \quad (26)$$

a vectorized multi-population state which contains all entries of $W \in \mathcal{W} \subseteq \mathbb{R}^{n \times c}$ stacked row-wise. Table 1 summarizes the scenarios discussed in the following.

Table 1: Structure of payoff (29) for simple instances of different games.

	S-Flow	EGN	Multi-Game
Payoff	$\bar{A} = \Omega \otimes \mathbb{I}_c$	$\bar{A} = \Omega \otimes B$	$\bar{A} = \mathbb{I}_n \otimes B$

S-flows (Savarino and Schnörr, 2020) define payoff by averaging the state S according to a weighted graph adjacency matrix $\Omega \in \mathbb{R}^{n \times n}$. The resulting assignment flow with vectorized state (26) reads

$$\dot{s}(t) = \mathcal{R}_{s(t)}[(\Omega \otimes \mathbb{I}_c)s(t)], \quad s(0) = s_0. \quad (27)$$

This dynamical system promotes similarity of adjacent populations. Depending on the initialization s_0 , ‘pockets of consensus’ are formed. It has also been shown that these dynamics converge to extremal points of \mathcal{W} for almost all initializations under weak conditions (Zern et al, 2022).

Evolutionary Games on Networks (EGN) (Madeo and Mocenni, 2015; Iacobelli et al, 2016) are dynamics which generalize (27) by incorporating payoff matrices for games played between players of adjacent populations. In the simplest case, all such games have a constant payoff matrix $B \in \mathbb{R}^{c \times c}$. Then, the multi-population replicator dynamics of EGN read

$$\dot{s}(t) = \mathcal{R}_{s(t)}[(\Omega \otimes B^\top)s(t)], \quad s(0) = s_0. \quad (28)$$

Both (27) and (28) have a linear (in the vectorized state s) payoff function. Let

$$\bar{A} \in \mathbb{R}^{nc \times nc} \quad (29)$$

be an arbitrary payoff matrix for the vectorized state. Then by Lemma 3.4 and Theorem 3.5, the embedded dynamics in $\mathcal{T} \subseteq \mathcal{S}_N$ read

$$\dot{p}(t) = R_{p(t)}[Q\bar{A}Q^\top p(t)], \quad p(0) = T(s_0). \quad (30)$$

The *multi-game dynamics* of Hashimoto (2006) can also be written as a matrix game in \mathcal{S}_N . Given matrices $A^{(i)} \in \mathbb{R}^{c \times c}$, $i \in [n]$, it reads

$$\dot{p}(t) = R_{p(t)}[Ap(t)], \quad p(0) = p_0, \quad A_{\alpha,\beta} = \sum_{i \in [n]} A_{\alpha_i,\beta_i}^{(i)}. \quad (31)$$

The structure of this payoff matrix has a natural shape within our formalism, too.

Lemma 4.1. *The payoff matrix in (31) can be written as $A = Q\bar{A}Q^\top$ where \bar{A} denotes the block diagonal matrix with diagonal blocks $A^{(i)}$.*

Proof.

$$(Q\bar{A}Q^\top)_{\alpha,\beta} = \langle e_\alpha, Q\bar{A}Q^\top e_\beta \rangle = \langle Q^\top e_\alpha, \bar{A}Q^\top e_\beta \rangle \quad (32a)$$

$$= \sum_{i \in [n]} \langle e_{\alpha_i}, A^{(i)} e_{\beta_i} \rangle = \sum_{i \in [n]} A_{\alpha_i, \beta_i}^{(i)} \quad (32b)$$

□

In particular, if all single-game payoff submatrices are the same $A^{(i)} = B \in \mathbb{R}^{c \times c}$, then multi-game dynamics have payoff $\bar{A} = \mathbb{I}_n \otimes B$.

It was shown by Hashimoto (2006) that the multi-game dynamics (31) do not generally decompose into individual single-game dynamics, unless the initialization is on the *Wright manifold* (see Figure 2). The set $\mathcal{T} \subseteq \mathcal{S}_N$ defined by (18a) is a generalization of the Wright manifold for $n > 2$ and Theorem 3.5 generalizes the decomposition of multi-game dynamics to more than two populations. For $p(0) \in \mathcal{T}$, the dynamics (31) is the embedded dynamics of

$$\dot{s}(t) = \mathcal{R}_{s(t)}[\bar{A}s(t)], \quad s(0) = Mp(0) \quad (33)$$

by Lemma 4.1 and Theorem 3.5. Since \bar{A} is block diagonal, (33) is a collection of non-interacting single-game replicator dynamics

$$\dot{W}_i(t) = R_{W_i(t)}[A^{(i)}W_i(t)], \quad W_i(0) = (Mp(0))_i, \quad i \in [n] \quad (34)$$

in accordance with the findings of Hashimoto (2006) for the specific case $n = 2$.

5 Tangent Space Parameterization

Multi-population replicator dynamics evolve in the *curved* space \mathcal{W} and the usual parameterization in m -coordinates of information geometry is subject to simplex constraints on the state. With an eye toward numerical integration, it is desirable to instead parameterize replicator dynamics in a *flat* and *unconstrained* vector space. This was done in (Zeilmann et al, 2020) using Lie group methods.

Theorem 5.1 (Proposition 3.1 in (Zeilmann et al, 2020)). *The solution for multi-population replicator dynamics*

$$\dot{W}(t) = \mathcal{R}_{W(t)}[F(W(t))], \quad W(0) = W_0 \quad (35)$$

in \mathcal{W} admits the parameterization

$$W(t) = \exp_{\mathbf{1}_{\mathcal{W}}}(V(t)) \quad (36a)$$

$$\dot{V}(t) = \Pi_0 F(\exp_{\mathbf{1}_{\mathcal{W}}}(V(t))), \quad V(0) = \Pi_0 \log W_0 \quad (36b)$$

in the tangent space $V(t) \in T_0\mathcal{W}$.

With regard to the Embedding Theorem 3.5, it turns out that while T maps assignment matrices $W \in \mathcal{W}$ to joint states $p \in \mathcal{S}_N$, Q assumes a corresponding role for tangent vectors in $T_0\mathcal{W}$.

Theorem 5.2 (Tangent Space Embedding Theorem). *The multi-population tangent space replicator dynamics*

$$\dot{V} = \Pi_0 F(\exp_{\mathbf{1}_W}(V)), \quad V(0) = V_0 \quad (37)$$

on $T_0\mathcal{W}$ is pushed forward by Q to the tangent space replicator dynamics

$$\dot{U} = \Pi_0 \hat{F}(\exp_{\mathbf{1}_N}(U)), \quad U(0) = Q(V_0), \quad \hat{F} = Q \circ F \circ M \quad (38)$$

on $T_0\mathcal{S}_N$.

Proof. Denoting $U = QV$ and using the lifting map (Lemma 3.3), we directly compute

$$\dot{U} = Q\dot{V} = Q\Pi_0 F(\exp_{\mathbf{1}_W}(V)) \quad (39a)$$

$$= \Pi_0 QF(\exp_{\mathbf{1}_W}(V)) \quad \text{by Lemma A.3} \quad (39b)$$

$$= \Pi_0 QF((M \circ T)(\exp_{\mathbf{1}_W}(V))) \quad \text{by (19)} \quad (39c)$$

$$= \Pi_0 QF(M \exp_{\mathbf{1}_N}(QV)) \quad \text{by Lemma 3.3} \quad (39d)$$

$$= \Pi_0 QF(M \exp_{\mathbf{1}_N}(U)) \quad (39e)$$

$$= \Pi_0 \hat{F}(\exp_{\mathbf{1}_N}(U)). \quad (39f)$$

□

Pushforward via Q thus preserves the shape of (37) up to the same fitness function transformation $\hat{F} = Q \circ F \circ T^{-1}$ from Theorem 3.5.

The set $\text{img } Q \subseteq T_0\mathcal{S}_N$ contains exactly those tangent vectors corresponding to assignments $\mathcal{T} \subseteq \mathcal{S}_N$ via lifting, because $T(W) = T(\exp_{\mathbf{1}_W}(V)) = \exp_{\mathbf{1}_N}(QV)$ for any $W \in \mathcal{W}$ and $V = \exp_{\mathbf{1}_W}^{-1}(W)$ by Lemma 3.3. In particular, the set $\text{img } Q$ in which U evolves, is a linear subspace of $T_0\mathcal{W}$. This is a reason to study the tangent space flow (38) rather than the corresponding replicator dynamics if applicable, because $\mathcal{T} \subseteq \mathcal{S}_N$ is the (curved) set of rank-1 tensors in \mathcal{S}_N .

6 Learning Replicator Dynamics from Data

Several applications have been proposed for the replicator dynamics of Section 4 including as a model of human brain functioning (Madeo et al, 2017), collective learning (Sato and Crutchfield, 2003), epileptic seizure onset detection (Hamavar and Asl, 2021), task mapping (Madeo et al, 2020) and collective adaptation (Sato et al, 2005). Assignment flows have been applied recently to the segmentation of digitized volume data under layer ordering constraints (Sitenko et al, 2021) (which reflect prior knowledge about tissues and anatomical structure) as well as for unsupervised image labeling tasks, employing spatial regularization (Zisler et al, 2020; Zern et al, 2020).



Fig. 3: *Left:* Noisy input assignment of $c = 47$ colors to the pixels of an image. *Center:* Limit of an EGN flow (28) with *learned* interaction in 3×3 pixel neighborhoods. *Right:* Ground truth noise-free color assignment.

This small sample of examples illustrates that replicator dynamics can act as powerful data models in diverse applications. In situations where only partial knowledge about the system is available, system parameters may also be learned from data. To this end, Hühnerbein et al (2020) have studied the use of *adjoint integration* to compute the model sensitivity of assignment flows, i.e. the gradient of system state with respect to parameters generating the flow.

Suppose we integrate a general dynamical system generated by parameters \mathbf{p} and wish for the final state $v(T)$ to minimize some loss function \mathcal{L} . The parameter learning problem for a fixed time horizon $T > 0$ then reads

$$\min_{\mathbf{p}} \mathcal{L}(v(T, \mathbf{p})) \quad (40a)$$

$$\text{subject to } \dot{v}(t) = f(v(t), \mathbf{p}, t), \quad t \in [0, T], \quad (40b)$$

$$v(0) = v_0, \quad (40c)$$

and a central quantity of interest is the gradient $\partial_{\mathbf{p}} \mathcal{L}(v(T, \mathbf{p}))$. It can be approximated in a *discretize-then-optimize* fashion by first choosing a discretization of the ODE (40b) on $[0, T]$ and subsequently computing the gradient of the discrete scheme used for computing $\mathcal{L}(v(T, \mathbf{p}))$. This approach is easy to implement by using automatic differentiation software Baydin et al (2018). However, it entails a large memory footprint in practical applications because system state $v(t_i)$ needs to be saved for all discretization points. To circumvent this issue, one may instead proceed in an *optimize-then-discretize* fashion as follows.

Theorem 6.1 (Theorem 6 of (Hühnerbein et al, 2020)). *The gradient of (40) is given by*

$$\partial_{\mathbf{p}} \mathcal{L}(v(T, \mathbf{p})) = \int_0^T d_{\mathbf{p}} f(v(t), \mathbf{p}, t)^\top \lambda(t) dt \quad (41)$$

where $d_{\mathbf{p}} f$ denotes the differential of f with respect to \mathbf{p} and $x(t)$ and $\lambda(t)$ solve

$$\dot{v}(t) = f(v(t), \mathbf{p}, t), \quad v(0) = v_0, \quad (42a)$$

$$\dot{\lambda}(t) = -d_v f(v(t), \mathbf{p}, t)^\top \lambda(t), \quad \lambda(T) = \partial \mathcal{L}(v(T)). \quad (42b)$$

By choosing a quadrature for the integral (41), Theorem 6.1 allows to compute the desired gradient without the need to save system state at all discretization points. Moreover, it has been shown (Hühnerbein et al, 2020; Sanz-Serna, 2016) that for particular *symplectic* integrators, discretization commutes with optimization, i.e. both orders of operation yield the same gradient.

Since the tangent space parameterization (36) evolves on the unconstrained flat space $T_0\mathcal{W}$, Theorem 6.1 is directly applicable to it. An image labeling example is shown in Figure 3. Here, the data is modeled by EGN dynamics (28) with graph adjacency matrix Ω representing pixel neighborhoods (3×3). Starting from a noisy, high-entropy assignment of pixels to color prototypes ($c = 47$), the goal is to learn a label interaction matrix $B \in \mathbb{R}^{c \times c}$ such that EGN dynamics (28) drive the state to a given noise-free assignment after the fixed integration time $T = 15$. We initialized B as identity matrix and performed 100 steps of the Adam optimizer to minimize cross-entropy between the ground truth assignment and the assignment state reached by EGN dynamics. This training procedure is highly scalable – for the 256×256 pixel image in Figure 3, training takes less than a minute on a laptop computer and requires around 1.3GB of vRAM.

7 Asymptotic Behavior

A central topic in population dynamics is the study of how the properties of the underlying game characterized by the payoff function relate to steady states of the dynamical model. In this section, we describe how

- *Nash equilibria (NE)* and
- *Evolutionarily stable states (ESS)*

of multi-population games and their replicator dynamics behave under the embedding (18a). Nash equilibria for multi-population games are population states at which no agent (in any population) has payoff to gain from unilaterally switching strategies.

Definition 7.1 (Nash Equilibrium). Let $\overline{\mathcal{W}}$, the closure of \mathcal{W} be the set of multi-population states (n populations, c strategies) and let $F: \overline{\mathcal{W}} \rightarrow \mathbb{R}^{n \times c}$ be the payoff for a multi-population game. The set of Nash equilibria of F is defined as

$$\text{NE}(F) = \{W \in \overline{\mathcal{W}} \mid \forall i \in [n], \forall j \in \text{supp}(W_i), \forall k \in [c] : F(W)_{i,j} \geq F(W)_{i,k}\} \quad (43)$$

Definition 7.1 naturally extends the classic notion of Nash equilibrium to multi-population games. Nash equilibria are preserved if the multi-population game is embedded as specified by Theorem 3.5.

Theorem 7.2 (Embedded Nash Equilibria). Let $F: \overline{\mathcal{W}} \rightarrow \mathbb{R}^{n \times c}$ be a multi-population game on $\overline{\mathcal{W}}$ and $\hat{F} = Q \circ F \circ M$ be the related population game on \mathcal{S}_N . Then

$$T(\text{NE}(F)) = \text{NE}(\hat{F}) \cap \overline{\mathcal{T}}. \quad (44)$$

Proof. Let $W \in \text{NE}(F)$ and let $\alpha \in \text{supp}(T(W))$ be arbitrary. Then

$$\widehat{F}(T(W))_\alpha = (QF(W))_\alpha = \sum_{l \in [n]} F_{l, \alpha_l}(W) \quad (45a)$$

$$\geq \sum_{l \in [n]} F_{l, \beta_l}(W) = \widehat{F}(T(W))_\beta, \quad \forall \beta \in [c]^n, \quad (45b)$$

because $\alpha_l \in \text{supp}(W_l)$, $\forall l \in [n]$, by Lemma A.2 and W is a Nash equilibrium of F . This implies $T(\text{NE}(F)) \subseteq \text{NE}(\widehat{F}) \cap \overline{\mathcal{T}}$. Conversely, let $p \in \text{NE}(\widehat{F}) \cap \mathcal{T}$ have shape $p = T(W)$ and let $\alpha_l \in \text{supp}(W_l)$, $\forall l \in [n]$. Then $\alpha \in \text{supp}(p)$ by Lemma A.2 and

$$\sum_{l \in [n]} F_{l, \alpha_l}(W) = \widehat{F}(p)_\alpha \geq \widehat{F}(p)_\beta = \sum_{l \in [n]} F_{l, \beta_l}(W), \quad \forall \beta \in [c]^n, \quad (46)$$

because p is a Nash equilibrium. Choose $\beta \in [c]^n$ such that it matches α at all positions but $i \in [n]$. Then (46) implies $F_{i, \alpha_i}(W) \geq F_{i, \beta_i}(W)$ for arbitrary $\beta_i \in [c]$ which shows $\text{NE}(\widehat{F}) \cap \overline{\mathcal{T}} \subseteq T(\text{NE}(F))$. \square

Definition 7.3 (Evolutionarily Stable State (ESS)). A multi-population state $W^* \in \mathcal{W}$ is called an evolutionarily stable state (ESS) of a game $F: \mathcal{W} \rightarrow \mathbb{R}^{n \times c}$, if there is an environment $U \subseteq \mathcal{W}$ of W^* such that

$$\langle W - W^*, F(W) \rangle < 0, \quad \forall W \in U \setminus \{W^*\}. \quad (47)$$

This generalization of the classic ESS (Smith and Price, 1973) to multi-population settings is called *Taylor ESS* by Sandholm (2010). Within our embedding framework, an apparent reason recommends Definition 7.3 over the weaker notion of *monomorphic ESS* (Cressman, 1992).

Theorem 7.4 (Embedded ESS). Let $F: \mathcal{W} \rightarrow \mathbb{R}^{n \times c}$ be a multi-population game. Then W^* is an ESS of F exactly if there exists an environment $U \subseteq \mathcal{T}$ of $T(W^*)$ such that

$$\langle p - T(W^*), \widehat{F}(p) \rangle < 0, \quad \forall p \in U \setminus \{T(W^*)\}, \quad (48)$$

where $\widehat{F} = Q \circ F \circ M$ denotes the embedded single-population game on \mathcal{S}_N as specified by Theorem 3.5.

Proof. Since $U \subseteq \mathcal{T}$, we may write $p = T(W)$ for W in an environment $M(U) \subseteq \mathcal{W}$ of W^* . (48) then reads

$$\langle T(W) - T(W^*), \widehat{F}(T(W)) \rangle = \langle T(W) - T(W^*), QF(MT(W)) \rangle \quad (49a)$$

$$= \langle M(T(W) - T(W^*)), F(W) \rangle \quad (\text{Lemma 3.4}) \quad (49b)$$

$$= \langle W - W^*, F(W) \rangle \quad (49c)$$

and the last row is strictly smaller than 0 for all $W \in M(U) \setminus \{W^*\}$ exactly if W^* is an ESS of F according to Definition 7.3. \square

One useful aspect of Theorem 3.5 is that it formally reduces multi-population replicator dynamics to single-population ones. This enables us to transfer analysis of e.g. asymptotic behavior from the single-population to the multi-population setting. We first summarize standard results on the asymptotic behavior of replicator dynamics derived from a potential function and refer to Sandholm (2010) for a comprehensive overview.

Theorem 7.5 (Replicators converge to NE). *Let $\hat{J}: \mathcal{S}_c \rightarrow \mathbb{R}$ be a C^1 potential such that the induced payoff function $\hat{F} = \Pi_0 \nabla \hat{J}$ is Lipschitz on \mathcal{S}_c . Then for any internal point $p_0 \in \mathcal{S}_c$, the replicator dynamics*

$$\dot{W}(t) = R_{p(t)}[\hat{F}(p)], \quad p(0) = p_0 \quad (50)$$

converge to a Nash equilibrium.

Proof. Because F is Lipschitz, the forward trajectories of the dynamics (50) are unique by the Picard-Lindelöf theorem. The potential \hat{J} is a strict Lyapunov function for replicator dynamics and unique forward trajectories converge to restricted equilibria (Hofbauer, 2001; Sandholm, 2001). Since replicator dynamics do not satisfy Nash stationarity, there may be restricted equilibria which are not Nash equilibria. However, no internal trajectory converges to any of these points (Bomze, 1986). The solution trajectories of (50) are internal trajectories because p_0 is an internal point and \mathcal{S}_c is invariant under all replicator dynamics with Lipschitz payoff function for finite time, as is clear from e.g. the tangent space parameterization (36). \square

There is a simple relationship between potential functions in the multi-population and single-population settings.

Lemma 7.6 (Potential Embedding). *If $F: \mathcal{W} \rightarrow T_0 \mathcal{W}$ has potential J , then $\hat{F} = Q \circ F \circ M$ has potential $\hat{J} = J \circ M$.*

Proof. For $\hat{J}(p) = (J \circ M)(p)$, we directly compute

$$\nabla \hat{J}(p) = (DM(p))^\top \nabla J(W) = (M)^\top \circ \nabla J(W) = (Q \circ \nabla J \circ M)(p) \quad (51)$$

by denoting $W = M(p)$ and using Lemma 3.4. \square

We can now use the embedded potential of Lemma 7.6 and embedded Nash equilibria of Theorem 7.2 to generalize the findings of Theorem 7.5 to multiple populations.

Theorem 7.7 (Multi-Population Replicators converge to NE). *Let $J: \mathcal{W} \rightarrow \mathbb{R}$ be a C^1 potential such that the induced payoff function $F = \Pi_0 \nabla J$ is Lipschitz on \mathcal{W} . Then, for any internal point $W_0 \in \mathcal{W}$, the multi-population replicator dynamics*

$$\dot{W}(t) = \mathcal{R}_{W(t)}[F(W)], \quad W(0) = W_0 \quad (52)$$

converge to a Nash equilibrium.

Proof. Let $p(t) = T(W(t))$. Then $p(t)$ follows the single-population replicator dynamics (24) by Theorem 3.5 which are induced by the embedded potential $\hat{J}(p) = J \circ M$ due to Lemma 7.6 and start at the interior point $T(W_0)$ of \mathcal{S}_N . By Theorem 7.5, $p(t)$ converges to a NE of $\hat{F} = \Pi_0 \circ Q \circ F \circ M$ on \mathcal{S}_N . Since $p(t) = T(W(t)) \in \mathcal{T}$ for all times t , the limit point necessarily lies in the closure of \mathcal{T} . Theorem 7.2 then shows the assertion. \square

By (Sandholm, 2001, Proposition 3.1) all Nash equilibria satisfy the KKT optimality conditions for maximizing J subject to simplex constraints. If J is concave, the KKT conditions are sufficient optimality conditions and thus (50) converges to a local maximizer. In addition, W is a Nash equilibrium exactly if $F(W)$ lies in the normal cone of the state space at W (Harker and Pang, 1990; Nagurney, 1998). Thus, convergence of (50) to a boundary point which is not an extremal point only occurs if the trajectory reaches the boundary exactly perpendicularly. For assignment flows, it has been known that convergence to a non-extremal point of \mathcal{W} is an unusual occurrence. In fact, this behavior is not observed at all in the numerical solution of labeling problems for real-world data. Aström et al (2017) thus conjectured that convergence to a non-extremal point only occurs for a null set of initial population states. This was shown to be true for non-negative, linear fitness functions derived from a quadratic potential (Zern et al, 2022). From a game-theoretical perspective, only extremal points can be ESS under the posed conditions.

Note that the content of Theorem 7.7 is likely known to experts. We present it here to illustrate the power of the proposed formalism around Theorem 3.5 which provides a mathematical toolset for reducing the analysis of multi-population replicator dynamics to single-population ones.

8 Conclusion

The proposed embedding framework for multi-population replicator dynamics provides a robust mathematical toolset for modeling complex population interactions. It formally reduces the complex multi-population case to a single-population one, simplifying subsequent analysis. Current developments in the framework of assignment flows suggest multiple extensions of the present work.

In Savarino et al (2023), assignment flows are characterized as critical points of an action functional within a geometric formalism of mechanics. An analogous characterization was previously suggested for single-population replicator dynamics (Raju and Krishnaprasad, 2018) under assumptions which are valid only in the special case $n = 2$ (Savarino et al, 2023, Section 4.4). In light of the present paper, a natural question is whether both perspectives are equivalent under embedding of the multi-population case.

A generalized perspective on assignment flows was proposed by Schwarz et al (2023). The authors study a dynamical system on a product of density matrix manifolds called *Quantum State Assignment Flow*. Although density matrices can represent entangled states and constitute a strict generalization of discrete probability measures, the underlying information geometric framework is broadly analogous. This suggests

that generalized, quantum embedding results, along the lines introduced in the present paper, should be achievable.

We briefly elaborate this point. Quantum mechanics is formulated on complex projective space $\mathbb{P}(\mathbb{C}^c) = \mathbb{P}^{c-1}$, i.e. the state of an c -dimensional quantum system lives in the $(c-1)$ -dimensional projective space. The states of a composite quantum system with n components comprise the space $\mathbb{P}(\bigotimes_{i=1}^n \mathbb{C}^c) \cong \mathbb{P}^{N-1}$, the projective space of the tensor products and $N = c^n$. The Segre embedding σ (Smith et al, 2000) is an analytic isometric embedding of products of projective spaces into higher dimensional projective space (Chen, 2013), i.e.

$$\sigma : \mathbb{P}^{c-1} \times \dots \times \mathbb{P}^{c-1} \hookrightarrow \mathbb{P}^{N-1}, \quad (53)$$

where the product contains n copies of \mathbb{P}^{c-1} . The map σ is an isometry if the product of projective spaces is equipped with the product of Fubini-Study metrics and the projective space of the tensor product with the high dimensional Fubini-Study metric. The *separable (unentangled) quantum states* of the composite system are precisely the image of the Segre embedding. Furthermore, \mathbb{P}^{c-1} admits a description as a toric variety with base Δ_c , the simplex with boundary (Bengtsson and Zyczkowski, 2017). Exploiting this structure makes it possible to choose compatible smooth embeddings

$$\iota : \mathcal{S}_c \times \dots \times \mathcal{S}_c \hookrightarrow \mathbb{P}^{c-1} \times \dots \times \mathbb{P}^{c-1}, \quad (54)$$

and to define a projection map $\pi_c : \mathbb{P}^{c-1} \rightarrow \Delta_c$. The embedding T given by (18a) is compatible with the Segre embedding σ in the sense that the diagram

$$\begin{array}{ccc} \mathbb{P}^{c-1} \times \dots \times \mathbb{P}^{c-1} & \xrightarrow{\sigma} & \mathbb{P}^{N-1} \\ \uparrow \iota & & \downarrow \pi_N \\ \mathcal{S}_c \times \dots \times \mathcal{S}_c & \xrightarrow{T} & \mathcal{S}_N \end{array} \quad (55)$$

is well-defined and commutes. Well-defined refers here to the fact that $\pi_N \circ \sigma \circ \iota$ maps to $\mathcal{S}_N \subset \Delta_N$. Additionally, similar compatibility relations remain valid when quantum states are described in terms of density matrices.

Elaborating the consequences of the results in this paper in connection with the more general quantum state assignment flow approach is an attractive research problem for future work.

Acknowledgments. The original artwork used in Figure 3 was designed by dgim-studio / Freepik.

The authors thank Fabrizio Savarino for many fruitful discussions and suggestions.

Declarations

Funding

This work is funded by the Deutsche Forschungsgemeinschaft (DFG), grant SCHN 457/17-1, within the priority programme SPP 2298: “Theoretical Foundations of Deep Learning”. This work is funded by the Deutsche Forschungsgemeinschaft (DFG) under Germany’s Excellence Strategy EXC-2181/1 - 390900948 (the Heidelberg STRUCTURES Excellence Cluster).

Competing interests

The authors have no relevant financial or non-financial interests to disclose.

References

- Amari Si, Nagaoka H (2007) *Methods of Information Geometry*, vol 191. American Mathematical Soc.
- Argasinski K (2006) Dynamic multipopulation and density dependent evolutionary games related to replicator dynamics. a metasimplex concept. *Mathematical biosciences* 202(1):88–114
- Aström F, Petra S, Schmitzer B, et al (2017) Image Labeling by Assignment. *J Math Imag Vision* 58(2):211–238
- Ay N, Jost J, Vân Lê H, et al (2017) *Information Geometry*, vol 64. Springer
- Baydin A, Pearlmutter B, Radul A, et al (2018) Automatic Differentiation in Machine Learning: a Survey. *J Machine Learning Research* 18:1–43
- Bednar J, Page S (2007) Can game(s) theory explain culture?: The emergence of cultural behavior within multiple games. *Rationality and Society* 19(1):65–97. <https://doi.org/10.1177/1043463107075108>
- Bengtsson I, Życzkowski K (2017) *Geometry of Quantum States: An Introduction to Quantum Entanglement*, 2nd edn. Cambridge University Press
- Boll B, Schwarz J, Schnörr C (2021) On the correspondence between replicator dynamics and assignment flows. In: Elmoataz A, Fadili J, Quéau Y, et al (eds) *Scale Space and Variational Methods in Computer Vision*. Springer International Publishing, Cham, pp 373–384
- Bollacker KD, Lawrence S, Giles CL (1998) Citeseer: An autonomous web agent for automatic retrieval and identification of interesting publications. In: *Proceedings of the second international conference on Autonomous agents*, pp 116–123
- Bomze IM (1986) Non-cooperative two-person games in biology: A classification. *International Journal of Game Theory* 15(1):31–57
- Chamberland M, Cressman R (2000) An example of dynamic (in)consistency in symmetric extensive form evolutionary games. *Games and Economic Behavior* 30(2):319–326
- Chen BY (2013) Segre embedding and related maps and immersions in differential geometry. URL <http://arxiv.org/abs/1307.0459>, 1307.0459[math]
- Cressman R (1992) *The stability concept of evolutionary game theory: a dynamic approach*, vol 94. Springer
- Cressman R, Tao Y (2014) The replicator equation and other game dynamics. *Proceedings of the National Academy of Sciences* 111(supplement_3):10810–10817

- Drton M, Sturmfels B, Sullivant S (2009) Lectures on Algebraic Statistics. Birkhäuser Basel, Basel
- Gardner RJ (2003) Games for business and economics, 2nd edn. Wiley, Hoboken, NJ
- Görtz U, Wedhorn T (2020) Algebraic Geometry I: Schemes: With Examples and Exercises. Springer Studium Mathematik - Master, Springer Fachmedien, Wiesbaden
- Graham A (1981) Kronecker Products and Matrix Calculus: with Applications. Ellis Horwood Limited
- Hamavar R, Asl BM (2021) Seizure onset detection based on detection of changes in brain activity quantified by evolutionary game theory model. *Computer Methods and Programs in Biomedicine* 199:105899
- Hammerstein P, Selten R (1994) Game theory and evolutionary biology. In: *Handbook of Game Theory with Economic Applications*, vol 2. Elsevier, p 929–993
- Harker PT, Pang JS (1990) Finite-dimensional variational inequality and nonlinear complementarity problems: A survey of theory, algorithms and applications. *Mathematical Programming* 48(1):161–220
- Hashimoto K (2006) Unpredictability induced by unfocused games in evolutionary game dynamics. *Journal of Theoretical Biology* 241(3):669–675
- Hofbauer J (2001) From nash and brown to maynard smith: Equilibria, dynamics and ess. *Selection* 1(1-3):81 – 88
- Hofbauer J, Sigmund K (1998) *Evolutionary games and population dynamics*. Cambridge university press
- Hühnerbein R, Savarino F, Petra S, et al (2020) Learning Adaptive Regularization for Image Labeling Using Geometric Assignment. *J Math Imaging Vision*
- Hühnerbein R, Savarino F, Petra S, et al (2021) Learning Adaptive Regularization for Image Labeling Using Geometric Assignment. *J Math Imaging Vision* 63:186–215
- Iacobelli G, Madeo D, Mocenni C (2016) Lumping evolutionary game dynamics on networks. *Journal of Theoretical Biology* 407:328–338
- Jost J (2017) *Riemannian Geometry and Geometric Analysis*, 7th edn. Springer
- Lee JM (2018) *Introduction to Riemannian Manifolds*, vol 2. Springer
- Leimar O, McNamara JM (2023) Game theory in biology: 50 years and onwards. *Philosophical Transactions of the Royal Society B: Biological Sciences* 378(1876):20210509

- Madeo D, Mocenni C (2015) Game interactions and dynamics on networked populations. *IEEE Transactions on Automatic Control* 60(7):1801–1810
- Madeo D, Talarico A, Pascual-Leone A, et al (2017) An evolutionary game theory model of spontaneous brain functioning. *Scientific reports* 7(1):1–11
- Madeo D, Mazumdar S, Mocenni C, et al (2020) Evolutionary game for task mapping in resource constrained heterogeneous environments. *Future Generation Computer Systems* 108:762–776
- Nagurney A (1998) *Network economics: A variational inequality approach*, vol 10. Springer Science & Business Media
- Nowak MA (2006) *Evolutionary Dynamics: Exploring the Equations of Life*. Harvard Univ. Press
- Raju V, Krishnaprasad P (2018) A Variational Problem on the Probability Simplex. In: 2018 IEEE Conf. on Decision and Control (CDC), IEEE, pp 3522–3528
- Samuelson L (2016) Game theory in economics and beyond. *Journal of Economic Perspectives* 30(4):107–130
- Sandholm WH (2001) Potential games with continuous player sets. *Journal of Economic Theory* 97(1):81–108
- Sandholm WH (2010) *Population games and evolutionary dynamics*. MIT press
- Sanz-Serna JM (2016) Symplectic runge–kutta schemes for adjoint equations, automatic differentiation, optimal control, and more. *SIAM Review* 58(1):3–33. <https://doi.org/10.1137/151002769>
- Sato Y, Crutchfield JP (2003) Coupled replicator equations for the dynamics of learning in multiagent systems. *Phys Rev E* 67:015206
- Sato Y, Akiyama E, Crutchfield JP (2005) Stability and diversity in collective adaptation. *Physica D: Nonlinear Phenomena* 210(1):21–57
- Savarino F, Schnörr C (2020) Continuous-Domain Assignment Flows. *Europ J Appl Math* pp 1–28
- Savarino F, Albers P, Schnörr C (2023) On the geometric mechanics of assignment flows for metric data labeling. *Information Geometry*
- Schnörr C (2020) Assignment Flows. In: Grohs P, Holler M, Weinmann A (eds) *Handbook of Variational Methods for Nonlinear Geometric Data*. Springer, p 235–260

- Schuster P, Sigmund K (1983) Replicator dynamics. *Journal of theoretical biology* 100(3):533–538
- Schwarz J, Cassel J, Boll B, et al (2023) Quantum state assignment flows. *Entropy* 25(9)
- Sitenko D, Boll B, Schnörr C (2021) Assignment Flow For Order-Constrained OCT Segmentation. *Int J Computer Vision* 129:3088–3118
- Smith JM (1982) Evolution and the theory of games. In: *Did Darwin get it right? Essays on games, sex and evolution*. Springer, p 202–215
- Smith JM, Price GR (1973) The logic of animal conflict. *Nature* 246(5427):15–18
- Smith KE, Kahanpää L, Kekäläinen P, et al (2000) *An Invitation to Algebraic Geometry*. Springer
- Taylor PD, Jonker LB (1978) Evolutionary stable strategies and game dynamics. *Mathematical biosciences* 40(1-2):145–156
- Venkateswaran VR, Gokhale CS (2019) Evolutionary dynamics of complex multiple games. *Proceedings of the Royal Society B: Biological Sciences* 286(1905):20190900
- Zeilmann A, Savarino F, Petra S, et al (2020) Geometric Numerical Integration of the Assignment Flow. *Inverse Problems* 36(3):034004 (33pp)
- Zeilmann A, Petra S, Schnörr C (2023) Learning Linearized Assignment Flows for Image Labeling. *J Math Imag Vision* 65:164–184
- Zern A, Zisler M, Petra S, et al (2020) Unsupervised Assignment Flow: Label Learning on Feature Manifolds by Spatially Regularized Geometric Assignment. *Journal of Mathematical Imaging and Vision* 62(6–7):982–1006
- Zern A, Zeilmann A, Schnörr C (2022) Assignment flows for data labeling on graphs: convergence and stability. *Information Geometry* 5(2):355–404
- Zisler M, Zern A, Petra S, et al (2020) Self-Assignment Flows for Unsupervised Data Labeling on Graphs. *SIAM Journal on Imaging Sciences* 13(3):1113–1156

Appendix A Additional Lemmata

Lemma A.1. *The mapping $T: \mathcal{W} \rightarrow \mathcal{T}$ defined by (18a) is injective.*

Proof. Let $W^{(1)}, W^{(2)} \in \mathcal{W}$ satisfy $T(W^{(1)}) = T(W^{(2)})$. Let $\gamma \in [c]^n$ be an arbitrary multi-index. Fix an arbitrary vertex $i \in [n]$ and let $\alpha \in [c]^n$ match γ at all vertices $k \in [n] \setminus \{i\}$. Then $T(W^{(1)}) = T(W^{(2)})$ implies both $T(W^{(1)})_\gamma = T(W^{(2)})_\gamma$ and $T(W^{(1)})_\alpha = T(W^{(2)})_\alpha$. Division thus gives

$$W_{i,\alpha_i}^{(1)} W_{i,\gamma_i}^{(2)} = W_{i,\gamma_i}^{(1)} W_{i,\alpha_i}^{(2)}. \quad (\text{A1})$$

Since $W^{(1)}, W^{(2)} \in \mathcal{W}$, the entries of row i sum to 1. Using this and the fact that $\alpha_i \in [c]$ is arbitrary, we find

$$W_{i,\gamma_i}^{(2)} = \sum_{j \in [c]} W_{i,j}^{(1)} W_{i,\gamma_i}^{(2)} \stackrel{(\text{A1})}{=} \sum_{j \in [c]} W_{i,\gamma_i}^{(1)} W_{i,j}^{(2)} = W_{i,\gamma_i}^{(1)}. \quad (\text{A2})$$

Since $\gamma_i \in [c]$ was arbitrary, this shows $W^{(1)} = W^{(2)}$. \square

Lemma A.2. *For every $W \in \overline{\mathcal{W}}$ one has $\gamma \in \text{supp}(T(W))$ if and only if $\gamma_i \in \text{supp}(W_i)$ for all $i \in [n]$.*

Proof. We directly compute

$$\text{supp}(T(W)) = \{\gamma \in [c]^n : T(W)_\gamma > 0\} \quad (\text{A3})$$

$$= \{\gamma \in [c]^n : \prod_{i \in [n]} W_{i,\gamma_i} > 0\} \quad (\text{A4})$$

$$= \{\gamma \in [c]^n : W_{i,\gamma_i} > 0, \forall i \in [n]\} \quad (\text{A5})$$

$$= \{\gamma \in [c]^n : \gamma_i \in \text{supp}(W_i), \forall i \in [n]\}. \quad (\text{A6})$$

\square

Lemma A.3. *For any $V \in \mathbb{R}^{n \times c}$ it holds $Q\Pi_0 V = \Pi_0 QV$ for the mappings Q, Π_0 given by (18b) and (14).*

Proof. For arbitrary $\gamma \in [c]^n$, we compute

$$(Q\Pi_0 V)_\gamma = \sum_{i \in [n]} (\Pi_0 V_i)_{\gamma_i} = \sum_{i \in [n]} (V_{i,\gamma_i} - \langle V_i, \frac{1}{c} \mathbf{1}_c \rangle) = (QV)_\gamma - \underbrace{\langle V, \frac{1}{c} \mathbf{1}_{n \times c} \rangle}_{=M\mathbf{1}_s} \quad (\text{A7})$$

and thus, by Lemma 3.4 ,

$$Q\Pi_0 V = QV - \langle QV, \frac{1}{N} \mathbf{1}_N \rangle \mathbf{1}_N = \Pi_0 QV, \quad (\text{A8})$$

which was the assertion. \square

Lemma A.4. Let $\gamma \in [c]^n$. The differential of T at $W \in \mathcal{W}$ in direction $V \in T_0\mathcal{W}$ is given by

$$dT|_W[V] = (dT_\gamma|_W[V])_{\gamma \in [c]^n} = T(W) \diamond Q \left[\frac{V}{W} \right]. \quad (\text{A9})$$

Proof. Suppose $\eta: (-\varepsilon, \varepsilon) \rightarrow \mathcal{W}$ is a smooth curve with $\eta(0) = W$ and $\dot{\eta}(0) = V$, for some $\varepsilon > 0$. Let $\gamma \in [c]^n$ be arbitrary and consider the component T_γ . Then

$$dT_\gamma|_W[V] = \frac{d}{dt} T_\gamma(\eta(t)) \Big|_{t=0} = \frac{d}{dt} \prod_{i \in [n]} \eta_{i, \gamma_i}(t) \Big|_{t=0} \quad (\text{A10a})$$

$$= \sum_{k \in [n]} \dot{\eta}_{k, \gamma_k}(0) \prod_{i \in [n] \setminus \{k\}} \eta_{i, \gamma_i}(0) = \sum_{k \in [n]} V_{k, \gamma_k} \prod_{i \in [n] \setminus \{k\}} W_{i, \gamma_i} \quad (\text{A10b})$$

$$= \sum_{k \in [n]} \frac{V_{k, \gamma_k}}{W_{k, \gamma_k}} T_\gamma(W) \stackrel{(\text{18b})}{=} T_\gamma(W) Q_\gamma \left(\frac{V}{W} \right). \quad (\text{A10c})$$

Because of $dT|_W[V] = (dT_\gamma|_W[V])_{\gamma \in [c]^n}$ the expression in (A9) directly follows. \square

Lemma A.5. It holds $\ker Q = \{\text{Diag}(d)\mathbf{1}_{n \times c} : d \in \mathbb{R}^n, \langle d, \mathbf{1}_n \rangle = 0\}$ as well as $\text{rank } Q = nc - (n - 1)$.

Proof. Let $V \in \ker Q$ and let $\gamma, \tilde{\gamma}$ be two multi-indices which differ exactly at position k but are otherwise arbitrary. We have $(QV)_\gamma = (QV)_{\tilde{\gamma}} = 0$ because $V \in \ker Q$. Thus

$$(QV)_{\tilde{\gamma}} = V_{k, \tilde{\gamma}_k} + \sum_{i \in [n] \setminus \{k\}} V_{i, \tilde{\gamma}_i} = (QV)_\gamma = V_{k, \gamma_k} + \sum_{i \in [n] \setminus \{k\}} V_{i, \gamma_i} \quad (\text{A11})$$

which implies $V_{k, \tilde{\gamma}_k} = V_{k, \gamma_k}$, i.e. $V = \text{Diag}(d)\mathbf{1}_{n \times c}$ for some $d \in \mathbb{R}^n$ since k was arbitrary. Further, it holds

$$0 = (QV)_\gamma = \sum_{i \in [n]} V_{i, \gamma_i} = \sum_{i \in [n]} d_i = \langle d, \mathbf{1}_n \rangle. \quad (\text{A12})$$

Thus, we have shown

$$\ker Q \subseteq \{\text{Diag}(d)\mathbf{1}_{n \times c} : d \in \mathbb{R}^n, \langle d, \mathbf{1}_n \rangle = 0\}. \quad (\text{A13})$$

Conversely, let V be in the right-hand set. Then

$$(QV)_\gamma = \sum_{i \in [n]} V_{i, \gamma_i} = \sum_{i \in [n]} d_i = \langle d, \mathbf{1}_n \rangle = 0 \quad (\text{A14})$$

for all $\gamma \in [c]^n$ which shows that (A13) is an equation. There are $(n - 1)$ linearly independent vectors $d \in \mathbb{R}^n$ with $\langle d, \mathbf{1}_n \rangle = 0$, therefore Q has the specified rank. \square

Appendix B Proofs

B.1 Proof of Theorem 3.1

Theorem B.1 (Theorem 3.1 in the main text). *The map $T: \mathcal{W} \rightarrow \mathcal{T}$ is an isometric embedding of \mathcal{W} equipped with product Fisher-Rao geometry into \mathcal{S}_N equipped with the Fisher-Rao geometry. On its image $T(\mathcal{W}) =: \mathcal{T} \subseteq \mathcal{S}_N$, the inverse is given by marginalization*

$$M|_{\mathcal{T}} = T^{-1}: \mathcal{T} \rightarrow \mathcal{W}. \quad (\text{B15})$$

Proof. A standard argument (Lemma A.1) shows that $T: \mathcal{W} \rightarrow \mathcal{T}$ is injective. We check that the inverse of T has the shape (19).

$$(MT(W))_{i,j} = \sum_{\gamma: \gamma_i=j} \prod_{r \in [n]} W_{r,\gamma_r} = \sum_{\gamma: \gamma_i=j} W_{i,j} \prod_{r \in [n] \setminus \{i\}} W_{r,\gamma_r} \quad (\text{B16})$$

$$= \sum_{l \in [n] \setminus \{i\}} \sum_{\gamma_l \in [c]} \prod_{r \in [n] \setminus \{i\}} W_{r,\gamma_r} \quad (\text{B17})$$

$$= W_{i,j} \sum_{k_1 \in [c]} W_{1,k_1} \sum_{k_2 \in [c]} W_{2,k_2} \cdots \sum_{k_n \in [c]} W_{n,k_n} \quad (\text{B18})$$

$$= W_{i,j} \prod_{r \in [n] \setminus \{i\}} \underbrace{\sum_{\gamma_r \in [c]} W_{r,\gamma_r}}_{=1} = W_{i,j}. \quad (\text{B19})$$

Clearly, all component functions of T and T^{-1} are smooth. We will now show that T is a topological embedding, i.e. a homeomorphism with respect to the subspace topology of $\mathcal{T} \subseteq \mathcal{S}_N$. Let

$$\mathcal{Q} = Q(T_0\mathcal{W}) \quad (\text{B20})$$

denote the image of $T_0\mathcal{W}$ under Q . \mathcal{Q} is a linear subspace of $T_0\mathcal{S}_N$ because, for any $V \in T_0\mathcal{W}$, we have

$$QV = Q\Pi_0V = \Pi_0QV \in T_0\mathcal{S}_N \quad (\text{B21})$$

by Lemma A.3. In addition, Lemma A.5 shows $\ker Q \cap T_0\mathcal{W} = \{0\}$, since any matrix in $\ker Q$ has constant row vectors. Thus, the restriction of Q to $T_0\mathcal{W}$ is injective and since $T_0\mathcal{W}$ and \mathcal{Q} have finite dimension, $Q|_{T_0\mathcal{W}}$ is a homeomorphism. The lifting map at the barycenter is the inverse of the *global* e -coordinate chart of information geometry up to a change of basis. In particular, $\exp_{\mathbf{1}_{\mathcal{W}}}: T_0\mathcal{W} \rightarrow \mathcal{W}$ and $\exp_{\mathbf{1}_{\mathcal{S}_N}}: T_0\mathcal{S}_N \rightarrow \mathcal{S}_N$ are homeomorphisms. Now let

$$\psi: \mathcal{T} \rightarrow \mathcal{Q}, \quad p \mapsto \psi(p) = \exp_{\mathbf{1}_{\mathcal{S}_N}}^{-1}(p) \quad (\text{B22})$$

which is well-defined due to Lemma 3.3 and denote the initial topology of \mathcal{T} with respect to ψ^{-1} by \mathcal{A} . Then T is a homeomorphism of \mathcal{W} and \mathcal{T} equipped with the topology \mathcal{A} because

$$T = \exp_{\mathbf{1}_{\mathcal{S}_N}} \circ Q|_{T_0\mathcal{W}} \circ \psi^{-1} \quad (\text{B23})$$

by Lemma 3.3. It remains to show that \mathcal{A} coincides with the subspace topology of $\mathcal{T} \subseteq \mathcal{S}_N$. Note that the topology of \mathcal{Q} is the subspace topology of $\mathcal{Q} \subseteq T_0\mathcal{S}_N$ and recall that $\exp_{\mathbf{1}_{\mathcal{S}_N}} : T_0\mathcal{S}_N \rightarrow \mathcal{S}_N$ is a homeomorphism. For a subset $A \subseteq \mathcal{Q}$ we thus have

$$A \in \mathcal{A} \Leftrightarrow \psi(A) \text{ is open in } \mathcal{Q} \quad (\text{B24a})$$

$$\Leftrightarrow \exp_{\mathbf{1}_{\mathcal{S}_N}}^{-1}(A) = B \cap \mathcal{Q} \text{ for an open set } B \subseteq T_0\mathcal{S}_N \quad (\text{B24b})$$

$$\Leftrightarrow \exp_{\mathbf{1}_{\mathcal{S}_N}}^{-1}(A) = \exp_{\mathbf{1}_{\mathcal{S}_N}}^{-1}(\bar{A}) \cap \mathcal{Q} \text{ for an open set } \bar{A} \subseteq \mathcal{S}_N \quad (\text{B24c})$$

$$\Leftrightarrow A = \bar{A} \cap \exp_{\mathbf{1}_{\mathcal{S}_N}}(\mathcal{Q}) \text{ for an open set } \bar{A} \subseteq \mathcal{S}_N \quad (\text{B24d})$$

$$\Leftrightarrow A = \bar{A} \cap \mathcal{T} \text{ for an open set } \bar{A} \subseteq \mathcal{S}_N. \quad (\text{B24e})$$

This shows that \mathcal{A} is the subspace topology of $\mathcal{T} \subseteq \mathcal{S}_N$ and thus, T is a topological embedding of \mathcal{W} into \mathcal{S}_N .

We compute the rank of T by applying Lemma A.4. Let $W \in \mathcal{W}$ and $V \in T_0\mathcal{W}$ be in the kernel of $dT|_W$. Then

$$0 = dT|_W[V] = T(W) \diamond Q\left[\frac{V}{W}\right] \quad (\text{B25})$$

which implies $\frac{V}{W} \in \ker Q$ because $T(W)_\gamma \neq 0$ for all $\gamma \in [c]^n$. By Lemma A.5 this implies

$$V = W \diamond (\text{Diag}(d)\mathbf{1}_{n \times c}) = \text{Diag}(d)W \quad (\text{B26})$$

for some $d \in \mathbb{R}^n$ with $\langle d, \mathbf{1}_n \rangle = 0$. From $V \in T_0\mathcal{W}$ we find

$$0 = \langle V_i, \mathbf{1}_c \rangle = d_i \langle W_i, \mathbf{1}_c \rangle = d_i, \quad \forall i \in [n] \quad (\text{B27})$$

which shows $V = 0$ by (B26), i.e. $dT|_W$ has full rank. Thus, T is an injective immersion.

It remains to show that T is metric compatible. Suppose $W \in \mathcal{W}$ and $U, V \in T_0\mathcal{W}$ are arbitrary. Denoting the Fisher-Rao metric on \mathcal{S}_N by $g^{\mathcal{S}_N}$ we get

$$(T^*g^{\mathcal{S}_N})_W(U, V) = g_{T(W)}^{\mathcal{S}_N}(dT|_W[U], dT|_W[V]) \quad (\text{B28a})$$

$$= \left\langle dT|_W[U], \frac{\mathbf{1}}{T(W)} \diamond dT|_W[V] \right\rangle \quad (\text{B28b})$$

$$\stackrel{(\text{A9})}{=} \left\langle dT|_W[U], Q\left[\frac{V}{W}\right] \right\rangle \quad (\text{B28c})$$

$$= \left\langle MdT|_W[U], \frac{V}{W} \right\rangle. \quad (\text{B28d})$$

Note that M is linear, implying $dM|_p = M$ for every $p \in \mathcal{S}_N$. Since M restricted to $\mathcal{T} = T(\mathcal{W})$ is the inverse of T , one has $M \circ T = \text{id}_{\mathcal{W}}$. These two facts imply

$$M[dT|_W[U]] = dM|_{T(W)}[dT|_W[U]] = d(M \circ T)|_W[U] = d(\text{id}_{\mathcal{W}})|_W[U] = U. \quad (\text{B29})$$

Plugging this result back into (B28d) gives

$$(T^*g^{\mathcal{S}_N})_W(U, V) = \left\langle U, \frac{V}{W} \right\rangle = g_W^{\mathcal{W}}(U, V) \quad (\text{B30})$$

which shows the assertion. \square

B.2 Proof of Proposition 3.2

Proposition B.2 (Proposition 3.2 in the main text). *For every $W \in \mathcal{W}$, the distribution $T(W) \in \mathcal{S}_N$ has maximum entropy among all $p \in \mathcal{S}_N$ subject to the marginal constraint $Mp = W$.*

Proof. We use the concepts of m-flat and e-flat submanifolds of information geometry, which justify applying the Pythagorean relation of information geometry. For details, we refer to Amari and Nagaoka (2007). The feasible set of all distributions with the prescribed marginals reads

$$\{T(W) + u: Mu = 0\} \cap \mathcal{S}_N \quad (\text{B31})$$

which is an m-flat submanifold of \mathcal{S}_N . In addition, Lemma 3.3 shows that \mathcal{T} is an e-flat submanifold of \mathcal{S}_N . Let $p = T(W) + u$ denote an arbitrary feasible point. By (B31) and Lemma 3.4 we have

$$\langle u, QV \rangle = \langle Mu, V \rangle = 0 \quad (\text{B32})$$

for all $V \in \mathbb{R}^{n \times c}$. Consider the m -geodesic connecting p with $T(W)$. It intersects \mathcal{T} at $T(W)$ and we find

$$\langle dT|_W[V], u \rangle = \langle T(W) \diamond Q\left[\frac{V}{W}\right], u \rangle_{T(W)} = \langle Q\left[\frac{V}{W}\right], u \rangle = \left\langle \frac{V}{W}, Mu \right\rangle = 0 \quad (\text{B33})$$

by using Lemma A.4. With (B33), m-flatness of (B31) and e-flatness of \mathcal{T} the prerequisites for the Pythagorean relation of information geometry (Amari and Nagaoka, 2007, Theorem 3.8) are met. Using the cross-entropy $H(p, q) = -\langle p, \log q \rangle$ as well as the relative entropy $\text{KL}(p, q) = \langle p, \log \frac{p}{q} \rangle$ and barycenter $\mathbf{1}_{\mathcal{S}_N} = \frac{1}{N}\mathbf{1}$, we find

$$\begin{aligned} H(T(W)) &= H(T(W), \mathbf{1}_{\mathcal{S}_N}) - \text{KL}(T(W), \mathbf{1}_{\mathcal{S}_N}) \\ &= \log N - \text{KL}(T(W), \mathbf{1}_{\mathcal{S}_N}) \end{aligned} \quad (\text{B34})$$

and consequently

$$H(p) = H(p, \mathbf{1}_{\mathcal{S}_N}) - \text{KL}(p, \mathbf{1}_{\mathcal{S}_N}) \quad (\text{B35})$$

$$= \log N - \text{KL}(p, \mathbf{1}_{\mathcal{S}_N}) \quad (\text{B36})$$

$$= H(T(W)) + \text{KL}(T(W), \mathbf{1}_{\mathcal{S}_N}) - \text{KL}(p, \mathbf{1}_{\mathcal{S}_N}) \quad (\text{B37})$$

$$\stackrel{(*)}{=} H(T(W)) + \text{KL}(T(W), \mathbf{1}_{\mathcal{S}_N}) - \text{KL}(p, T(W)) - \text{KL}(T(W), \mathbf{1}_{\mathcal{S}_N}) \quad (\text{B38})$$

$$= H(T(W)) - \text{KL}(p, T(W)) \quad (\text{B39})$$

by the Pythagorean relation (*). Therefore $H(p) \leq H(T(W))$ with equality only for $p = T(W)$ which shows the assertion. \square

B.3 Proof of Lemma 3.3

Lemma B.3 (Lifting Map Lemma). *Let $S \in \mathcal{W}$ and $V \in \mathbb{R}^{n \times c}$. Then*

$$T(\exp_S(V)) = \exp_{T(S)}(Q(V)). \quad (\text{B40})$$

Proof. We have $T(\exp(V)) = \exp(Q(V))$ (without subscripts, i.e. applying the exponential function componentwise), because for any multi-index γ

$$\exp(Q(V))_\gamma = \exp(Q(V)_\gamma) = \exp\left(\sum_{i \in [n]} V_{i, \gamma_i}\right) \quad (\text{B41a})$$

$$= \prod_{i \in [n]} \exp(V_{i, \gamma_i}) = \prod_{i \in [n]} (\exp(V))_{i, \gamma_i} \quad (\text{B41b})$$

$$= T(\exp(V))_\gamma. \quad (\text{B41c})$$

Let $D \in \mathbb{R}^{n \times n}$ be a diagonal matrix with nonzero diagonal entries. Then $T(DR) \propto T(R)$ for any $R \in \mathbb{R}^{n \times c}$ because

$$T(DR)_\gamma = \prod_{i \in [n]} (DR)_{i, \gamma_i} = \left(\prod_{i \in [n]} D_{ii}\right) \left(\prod_{i \in [n]} R_{i, \gamma_i}\right) \propto T(R)_\gamma. \quad (\text{B42})$$

It follows that

$$T(\exp_S(V)) \propto T(S \diamond \exp(V)) \stackrel{(\text{B41})}{=} T(S) \diamond \exp(Q(V)) \propto \exp_{T(S)}(Q(V)) \quad (\text{B43})$$

Because both the first and last term in (B43) are clearly elements of \mathcal{S}_N , i.e. strictly positive vectors summing up to 1, this implies the assertion. \square

B.4 Proof of Theorem 3.5

Theorem B.4 (Multi-Population Embedding Theorem). *For any payoff function $F: \mathcal{W} \rightarrow \mathbb{R}^{n \times c}$, the multi-population replicator dynamics*

$$\dot{W} = \mathcal{R}_W[F(W)], \quad W(0) = W_0 \quad (\text{B44})$$

on \mathcal{W} is pushed forward by T to the replicator dynamics

$$\dot{p}(t) = R_p(t) \hat{F}(p(t)), \quad p(0) = T(W_0), \quad \hat{F} = Q \circ F \circ M \quad (\text{B45})$$

on \mathcal{S}_N and the map T satisfies

$$dT|_W[\mathcal{R}_W[X]] = R_{T(W)}Q[X], \quad \text{for all } X \in \mathbb{R}^{n \times c} \text{ and } W \in \mathcal{W}. \quad (\text{B46})$$

Proof. We first show that, for any $W \in \mathcal{W}$, the differential of T and the replicator operator are related by (B46). Let $\gamma \in [c]^n$ be an arbitrary multi-index. Because of $\mathcal{R}_W[X] \in T_0\mathcal{W}$, Lemma A.4 implies

$$dT_\gamma|_W[\mathcal{R}_W[X]] = T_\gamma(W)Q_\gamma\left[\frac{\mathcal{R}_W[X]}{W}\right] = T_\gamma(W)\sum_{i \in [n]} \frac{(\mathcal{R}_W[X])_{i,\gamma_i}}{W_{i,\gamma_i}}. \quad (\text{B47})$$

Due to $(\mathcal{R}_W[X])_{i,\gamma_i} = W_{i,\gamma_i}(X_{i,\gamma_i} - \langle X_i, W_i \rangle)$, the sum can be written as

$$\sum_{i \in [n]} \frac{(\mathcal{R}_W[X])_{i,\gamma_i}}{W_{i,\gamma_i}} = \sum_{i \in [n]} (X_{i,\gamma_i} - \langle X_i, W_i \rangle) = Q_\gamma[X] - \langle X, W \rangle. \quad (\text{B48})$$

Additionally using the relation $W = M[T(W)]$ due to (B15), and applying Lemma 3.4 gives

$$\langle X, W \rangle = \langle X, M[T(W)] \rangle = \langle Q[X], T(W) \rangle. \quad (\text{B49})$$

Collecting all expressions, we have

$$dT_\gamma|_W[\mathcal{R}_W[X]] = T_\gamma(W)(Q_\gamma[X] - \langle Q[X], T(W) \rangle) = (R_{T(W)}Q[X])_\gamma \quad (\text{B50})$$

which shows (B46). Now, denoting $p = T(W) \in \mathcal{S}_N$ we directly establish (B45)

$$\dot{p} = dT(W)[\mathcal{R}_W[(F \circ M)(p)]] = R_p[(Q \circ F \circ M)(p)] = R_p[\widehat{F}(p)]. \quad (\text{B51})$$

□